JOURNAL OF GUIDANCE, CONTROL, AND DYNAMICS
Vol. 29, No. 2, March–April 2006

Nonlinear Adaptive Control of an Aeroelastic Two-Dimensional Lifting Surface

A. Behal,* P. Marzocca,† V. M. Rao,‡ and A. Gnann§
Clarkson University, Potsdam, New York 13699-5725

Adaptive control of a nonlinear two-dimensional wing-flap system operating in an incompressible flowfield is studied. An output feedback control law is implemented, and its performance toward suppressing flutter and limit cycle oscillations, as well as reducing the vibrational level in the subcritical flight speed range, is demonstrated. The control law proposed here is applicable to minimum phase systems, and conditions for stability of the zero dynamics are provided. The control objective is to design a control strategy to drive the pitch angle to a setpoint while adaptively compensating for uncertainties in all of the aeroelastic model parameters. It is shown that all of the states of the closed-loop system are asymptotically stable. Furthermore, an extension is presented to include flap actuator dynamics. Simulations have been presented to validate the efficacy of the proposed strategy. Pertinent conclusions have been outlined.

Nomenclature

b	=	semichord of airfoil
c_h, c_α	=	structural damping coefficients in plunge and pitch
$c_{l\alpha}$, $c_{m\alpha}$	=	lift and moment curve slopes per angle of attack
$c_{l\beta}$, $c_{m\beta}$	=	lift and moment curve slopes per control surface deflection
h	=	plunging displacement
I_α	=	mass moment of inertia of airfoil about elastic axis
k_h, k_α	=	structural spring stiffness in plunge and pitch
L	=	aerodynamic lift
M	=	aerodynamic moment
m	=	mass of airfoil
t	=	time
U	=	freestream velocity
x, y	=	horizontal and vertical coordinates
x_α	=	dimensionless distance from elastic axis to midchord, positive rearward
α	=	pitch angle
β	=	flap angle
ρ	=	air density

I. Introduction

FLUTTER instability can jeopardize aircraft performance and dramatically affect its survivability. Although flutter boundaries for an aircraft can be theoretically and experimentally determined, due to certain events occurring during its operational life, such as escape maneuvers, significant decays of the flutter speed are possible with dramatic implications for its structural integrity. Passive methods that have been used to address this problem include added structural stiffness, mass balancing, and speed restrictions.[1] However, all of these attempts to enlarge the operational flight envelope and to enhance the aeroelastic response result in significant weight penalties or in unavoidable reduction of nominal performances.[2,3] All of these factors fully underline the necessity of the implementation of an active control capability enabling one to fulfill the two basic objectives of 1) enhanced subcritical aeroelastic response, in the sense of suppressing or even alleviating the severity of the wing oscillations in the shortest possible time, and 2) expanded flight envelope by suppressing flutter instability, thereby contributing to a significant increase in the allowable flight speed.[4] The interest in the development and implementation of active control technology was prompted by the new and sometimes contradictory requirements imposed on the design of the new generation of the flight vehicle that mandated increasing structural flexibilities; high maneuverability; and, at the same time, the ability to operate safely in severe environmental conditions. In the last two decades, the advances of active control technology have rendered the applications of active flutter suppression and active vibrations control systems feasible.[5–11] A great deal of research activity devoted to the aeroelastic active control and flutter suppression of flight vehicles has been accomplished. The state-of-the-art advances in these areas are presented in Refs. 7–10 and 12.

Conventional methods of examining aeroelastic behavior have relied on a linear approximation of the governing equations of the flowfield and the structure. However, aerospace systems inherently contain structural and aerodynamic nonlinearities,[1,13] and it is well known that, with these nonlinearities present, an aeroelastic system may exhibit a variety of responses that are typically associated with nonlinear regimes of response, including limit cycle oscillation (LCO), flutter, and even chaotic vibrations.[12] These nonlinearities result from unsteady aerodynamic sources, such as those in transonic flow conditions or at high angle of attack, large deflections, and partial loss of structural or control integrity. Early studies have shown that the flutter instability can be postponed, and, consequently, the flight envelope can be expanded via implementation of a linear feedback control capability. However, the conversion of the catastrophic type of flutter boundary into a benign one requires the incorporation of a nonlinear feedback capability given a nonlinear aeroelastic system. In recent years, several active linear and nonlinear control capabilities have been implemented. Digital adaptive control of a linear aeroservoelastic model,[14] the μ method for robust aeroservoelastic stability analysis,[15] time-delayed feedback control,[11] gain scheduled controllers,[16] and neural and adaptive control of transonic wind-tunnel models[17,18] are only a few of the latest developed active control methods. Linear control theory, the feedback linearizing technique, and adaptive control strategies have been derived to account for the effect of nonlinear structural stiffness.[19–25] In their work on nonlinear and adaptive control, Zeng and Singh[22] propose a model reference variable structure adaptive control system for plunge displacement and pitch angle control using bounds on

Received 18 October 2004; revision received 24 January 2005; accepted for publication 25 January 2005.

*Assistant Professor, Electrical and Computer Engineering; abehal@clarkson.edu. Member AIAA.
†Assistant Professor, Mechanical and Aeronautical Engineering; pmarzocc@clarkson.edu. Member AIAA.
‡Student, Electrical and Computer Engineering; raovm@clarkson.edu.
§Student, Mechanical and Aeronautical Engineering; gnannal@clarkson.edu. Member AIAA.

uncertain functions. This approach yields a high-gain feedback discontinuous control system. In Ref. 24, an adaptive design method for flutter suppression has been adopted while using measurements of both the pitching and plunging variables.

In this paper, an adaptive control capability is implemented to regulate rapidly the pitching displacement to a setpoint while utilizing measurements of only the pitching displacement variable. Specifically, a bank of filters is designed to estimate the immeasurable state variables. These filter variables are then used to design a flap deflection control input in tandem with a gradient-based estimation scheme via the use of a Lyapunov function. Backstepping can be used to provide an extension to include the effect of manipulator dynamics.

In Sec. II, the system dynamics are introduced. In Sec. III, the control objective is described. Section IV deals with state estimation, control and adaptive update law design, along with stability analysis and signal chasing. In Sec. V, an extension to the control strategy is introduced that accounts for the dynamics of the flap. Section VI shows a comparison of the simulated results with some other published results. Conclusions are presented in Sec. VII.

II. Configuration of Two-Dimensional Wing Structural Model

Figure 1 shows a schematic for a plunging–pitching typical wing-flap section that is considered in the present analysis. This model has been widely used in aeroelastic analysis.[19–28] The plunging h and pitching α displacements are restrained by a pair of springs attached to the elastic axis (EA) of the airfoil with spring constants k_h and $k_\alpha(\alpha)$, respectively. Here, $k_\alpha(\alpha)$ denotes a continuous, linear parameterizable nonlinearity, that is, the aeroelastic system has a continuous nonlinear restoring moment in the pitch degree of freedom. Such continuous nonlinear models for stiffness result from a thin wing or propeller being subjected to large torsional amplitudes.[1,13] Similar models[19,20,22,23] have been examined and provide a basis for comparison. The aeroelastic system permits two degree-of-freedom (DOF) motion, whereas an aerodynamically unbalanced control surface is attached to the trailing edge. In addition to controlling the aerodynamic flow and providing increased maneuverability, the flap is used here to suppress instabilities. Here, h denotes the plunge displacement (positive downward), α the pitch angle (measured from the horizontal at the elastic axis of the airfoil, positive nose up), and β the aileron deflection (measured from the axis created by the airfoil at the control flap hinge, positive flap down). The governing equations of motion for the aeroelastic system under consideration are given by[19,20]

$$\begin{bmatrix} m & mx_\alpha b \\ mx_\alpha b & I_\alpha \end{bmatrix}\begin{bmatrix} \ddot{h} \\ \ddot{\alpha} \end{bmatrix} + \begin{bmatrix} c_h & 0 \\ 0 & c_\alpha \end{bmatrix}\begin{bmatrix} \dot{h} \\ \dot{\alpha} \end{bmatrix} + \begin{bmatrix} k_h & 0 \\ 0 & k_\alpha(\alpha) \end{bmatrix}\begin{bmatrix} h \\ \alpha \end{bmatrix} = \begin{bmatrix} -L \\ M \end{bmatrix} \tag{1}$$

where $k_\alpha(\alpha)$ denotes the pitch spring constant, a particular choice for which is presented in Sec. VI. As an example, the aerodynamic lift L and moment M can be modeled in a form as[29]

$$L = \rho U^2 b c_{l\alpha}\left[\alpha + \dot{h}/U + \left(\tfrac{1}{2} - a\right)b(\dot{\alpha}/U)\right] + \rho U^2 b c_{l\beta}\beta$$

$$M = \rho U^2 b^2 c_{m\alpha}\left[\alpha + \dot{h}/U + \left(\tfrac{1}{2} - a\right)b(\dot{\alpha}/U)\right] + \rho U^2 b^2 c_{m\beta}\beta \tag{2}$$

One can transform the governing equations of motion of Eq. (1) into the following equivalent state-space form as follows[20]:

$$\dot{\boldsymbol{z}} = \boldsymbol{f}(z) + \boldsymbol{g}(z)\beta, \qquad y = z_2 \tag{3}$$

where $\boldsymbol{z}(t) = [z_1\ z_2\ z_3\ z_4]^T \triangleq [h\ \alpha\ \dot{h}\ \dot{\alpha}]^T$ is a vector of system states, $\beta(t) \in \Re^1$ is a flap deflection control input, $y(t) \in \Re^1$ denotes the designated output, and $\boldsymbol{f}(z)$ and $\boldsymbol{g}(z) \in \Re^1$ assume the following form:

$$\boldsymbol{f}(z) = \begin{Bmatrix} z_3 \\ z_4 \\ -k_1 z_1 - \left[k_2 U^2 + p(z_2)\right]z_2 - c_1 z_3 - c_2 z_4 \\ -k_3 z_1 - \left[k_4 U^2 + q(z_2)\right]z_2 - c_3 z_3 - c_4 z_4 \end{Bmatrix}$$

$$\boldsymbol{g}(z) = \begin{Bmatrix} 0 \\ 0 \\ g_3 U^2 \\ g_4 U^2 \end{Bmatrix}, \qquad g_4 \neq 0 \tag{4}$$

where $p(z_2)$ and $q(z_2) \in \Re^1$ are continuous, linear parameterizable nonlinearities in the output variable resulting from the nonlinear pitch spring constant $k_\alpha(\alpha)$. The auxiliary constants k_i and $c_i\ \forall i = 1, \ldots, 4$, as well as g_3 and g_4, are explicitly defined in Appendix A. Motivated by the desire to rewrite Eq. (3) in a form that is amenable to output feedback control design, Kalman's observability test is applied to the pair $(\bar{\boldsymbol{A}}, \boldsymbol{C})$, where $\bar{\boldsymbol{A}} \in \Re^{4\times 4}$ and $\boldsymbol{C} \in \Re^{1\times 4}$ are explicitly defined as

$$\bar{\boldsymbol{A}} = \begin{bmatrix} 0 & 1 & 0 & 0 \\ -k_4 U^2 & -c_4 & -k_3 & -c_3 \\ 0 & 0 & 0 & 1 \\ -k_2 U^2 & -c_2 & -k_1 & -c_1 \end{bmatrix}, \qquad \boldsymbol{C} = \begin{bmatrix} 1 \\ 0 \\ 0 \\ 0 \end{bmatrix} \tag{5}$$

A sufficient condition for the system (3) to be observable from the pitch angle output $\alpha(t)$ is given as

$$d_{\text{obs}} = k_3^2 - k_3 c_3 c_1 + c_3^2 k_1 \neq 0$$

which is easily satisfied by the nominal model parameters of a two-DOF aeroelastic system presented in Sec. VI. After a series of coordinate transformations, the governing equations for the aeroelastic model can be expressed in the following convenient state-space form:

$$\dot{\boldsymbol{x}} = A\boldsymbol{x} + \boldsymbol{\Phi}(y) + B\bar{\beta}, \qquad y = \boldsymbol{C}^T\boldsymbol{x} = [1 \quad 0 \quad 0 \quad 0]\boldsymbol{x} \tag{6}$$

Herein, $\bar{\beta} = U^2\beta$ is an auxiliary control input, $\boldsymbol{x}(t) \in \Re^4$ is a new vector of system states, and $A \in \Re^{4\times 4}$ and $\boldsymbol{B} \in \Re^4$ are explicitly defined as

$$A = \begin{bmatrix} 0 & 1 & 0 & 0 \\ 0 & 0 & 1 & 0 \\ 0 & 0 & 0 & 1 \\ 0 & 0 & 0 & 0 \end{bmatrix}, \qquad B = \begin{bmatrix} 0 \\ \theta_2 \\ \theta_3 \\ \theta_4 \end{bmatrix} \tag{7}$$

where $\theta_i \forall i = 2, 3, 4$ are constants that are explicitly defined in Appendix A. In Eq. (6), $\boldsymbol{\Phi}(y) \in \Re^4$ is a smooth vector field that can be linearly parameterized as follows:

$$\boldsymbol{\Phi}(y) = W(y)\gamma = \sum_{j=1}^{p} \gamma_j W_j(y) \tag{8}$$

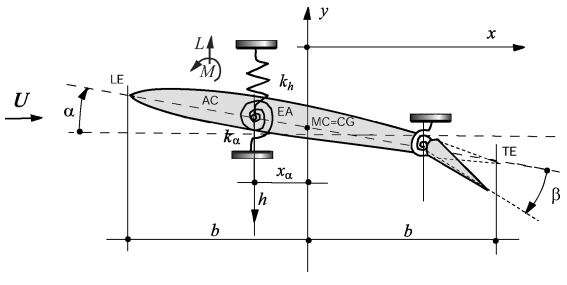

Fig. 1 Two-dimensional wing section aeroelastic model.

where $\gamma \in \Re^p$ is a vector of constant unknowns, $W(y) \in \Re^{4\times p}$ is a measurable, nonlinear regression matrix, and the notation $\boldsymbol{W}_j(\,) \in \Re^4$ denotes the jth column of the regression matrix $\boldsymbol{W}(\,) \forall j = 1, \ldots, p$. For a particular choice of the pitch spring nonlinearity $k_\alpha(\alpha)$, explicit expressions for γ in terms of model parameters are provided in Appendix A. As mentioned in Ref. 19, the model (3) is accurate for airfoils at low velocity and has been confirmed by wind-tunnel experiments. Following Ref. 19, unsteady aerodynamic modeling can also be implemented.[2,3,30–33] We also note that the proposed control strategy is predicated on the assumption that the system (6) is minimum phase. In Appendix B, the zero dynamics of the system are studied, and conditions for stability of the zero dynamics are provided.

III. Control Objective

Provided that the structures of both the aeroelastic model and the pitch spring constant nonlinearity are known, our objective is to design a controller to drive the pitch angle α to a constant setpoint while adaptively compensating for uncertainties in all parameters of the model and the nonlinearity. It is assumed that the only measurements available are those of the output variable $y = \alpha$, whereas compensation is provided for the remaining states via the use of state estimators. Toward these goals, the pitch angle setpoint error $e_1(t)$ and a state estimation error $\tilde{\boldsymbol{x}}(t)$ are defined as follows:

$$e_1 = y - y_d \tag{9}$$

$$\tilde{\boldsymbol{x}} = \boldsymbol{x} - \hat{\boldsymbol{x}} \tag{10}$$

where $\hat{\boldsymbol{x}}(t) \in \Re^4$ is a state estimate that is yet to be designed. Because the model parameters are assumed to be unknown, one can define parameter estimation error signals $\tilde{\boldsymbol{\sigma}}_0(t) \in \Re^{p_1}$ and $\tilde{\boldsymbol{\sigma}}_1(t) \in \Re^{p_2}$ as follows:

$$\tilde{\boldsymbol{\sigma}}_0 = \boldsymbol{\sigma}_0 - \hat{\boldsymbol{\sigma}}_0, \qquad \tilde{\boldsymbol{\sigma}}_1 = \boldsymbol{\sigma}_1 - \hat{\boldsymbol{\sigma}}_1 \tag{11}$$

where $\boldsymbol{\sigma}_0 \in \Re^{p_1}$ and $\boldsymbol{\sigma}_1 \in \Re^{p_2}$ are unknown constant vectors that will be subsequently explicitly defined, and $\hat{\boldsymbol{\sigma}}_0(t)$ and $\hat{\boldsymbol{\sigma}}_1(t)$ are their corresponding dynamic estimates that will be generated as part of a Lyapunov-based control design scheme. Note that p_1 and p_2 are non-negative integers whose values are determined through an explicit choice for the nonlinearity in the structural model.

IV. Estimation, Control, and Stability

Following the work in Ref. 22, we design the following bank of filters:

$$\dot{\zeta}_0 = A\zeta_0 + k\boldsymbol{C}^T(x - \zeta_0) \tag{12}$$

$$\dot{\boldsymbol{\zeta}}_j = A_0\boldsymbol{\zeta}_j + W_j(y), \qquad \forall j = 1, \ldots, p \tag{13}$$

$$\dot{\boldsymbol{\upsilon}}_i = A_0\boldsymbol{\upsilon}_i + \boldsymbol{\lambda}_i\bar{\beta}, \qquad \forall i = 2, 3, 4 \tag{14}$$

where $\boldsymbol{\lambda}_i$ denotes the standard basis vectors and A_0 is an auxiliary matrix defined as $A_0 = A - K_W C$ and $K_W = [40\ 600\ 4000\ 10{,}000]$. Given Eqs. (12–14), an immeasurable state estimate $\hat{\boldsymbol{x}}(t)$ can be patched together, as follows:

$$\hat{\boldsymbol{x}} = \zeta_0 + \sum_{j=1}^{p} \boldsymbol{\gamma}_j\boldsymbol{\zeta}_j + \sum_{j=2}^{4} \boldsymbol{\theta}_j\boldsymbol{\upsilon}_j \tag{15}$$

When the derivative of Eq. (10) is taken and the dynamics of Eqs. (6) and (15) are substitute for, the following exponentially stable estimation error system can be obtained:

$$\dot{\tilde{\boldsymbol{x}}} = A_0\tilde{\boldsymbol{x}} \tag{16}$$

Although the state estimate is immeasurable, the worth of the foregoing design lies in the linear parameterizability of the right-hand side of the expression (15), as well as the exponential stability of the estimation error.

Because the relative degree of the system is two, backstepping is required to reach the control input variable. In a state feedback setting, the choice of the virtual control would be x_2, but it is assumed to be immeasurable. Hence, one needs to backstep[34] on one of the filter variables defined in the preceding section. After taking the derivative of the regulation error $e_1(t)$, substituting Eq. (6) for the system dynamics, and adding and subtracting Eq. (15), one can obtain the open-loop error dynamics as follows:

$$\dot{e}_1 = \zeta_{0,2} + \sum_{j=1}^{p} \gamma_j[\zeta_{j,2} + W_{j,1}(y)] + \sum_{j=2}^{4} \theta_j\upsilon_{j,2} + \tilde{x}_2 \tag{17}$$

Similar to the case in Ref. 22, an auxiliary error signal $e_2(t) \in \Re^1$ is defined as $e_2 \triangleq \upsilon_{2,2} - \upsilon_{2,2,d}$ where $\upsilon_{2,2d}(t) \in \Re^1$ is a yet to be designed backstepping signal. After adding and subtracting $\upsilon_{2,2d}(t)$, as well as a feedback term $(-c_{11} - d_{11})e_1$ to the right-hand side of Eq. (17), and rearranging the terms in a manner amenable to the pursuant analysis, one obtains

$$\dot{e}_1 = \theta_2\left[\boldsymbol{\omega}_1^T\boldsymbol{\sigma}_0 + \upsilon_{2,2d}\right] - (c_{11} + d_{11})e_1 + \theta_2 e_2 + \tilde{x}_2 \tag{18}$$

where c_{11} and d_{11} are positive gain constants and σ_0 and $\omega_1(t) \in \Re^{p1}$ denote, respectively, a vector of unknown constants and a measurable regression vector, explicitly defined in Appendix A. Given the structure of Eq. (18), the desired backstepping signal $\upsilon_{2,2d}(t)$ can be designed as follows:

$$\upsilon_{2,2d} = -\boldsymbol{\omega}_1^T\hat{\boldsymbol{\sigma}}_0 \tag{19}$$

After substituting this control input into the open-loop expression of Eq. (18), one can obtain the following expression:

$$\dot{e}_1 = \theta_2\boldsymbol{\omega}_1^T\tilde{\boldsymbol{\sigma}}_0 - (c_{11} + d_{11})e_1 + \theta_2 e_2 + \tilde{x}_2 \tag{20}$$

where the definition of Eq. (11) has been utilized. From the structure of Eq. (20), a standard dynamic adaptive update law is chosen as $\dot{\hat{\sigma}}_0 = \text{sign}(\theta_2)\omega_1 e_1$. Our next step involves the design of our actual control input $\bar{\beta}(t)$, which is easily reachable through differentiation of $e_2(t)$ along the dynamics of Eq. (14) as follows:

$$\dot{e}_2 = -k_2\upsilon_{2,1} + \upsilon_{2,3} + \bar{\beta} - \dot{\upsilon}_{2,2d} \tag{21}$$

Before one designs for $\bar{\beta}$, one needs to separate out $\dot{\upsilon}_{2,2d}$ into its measurable and immeasurable components

$$\dot{\upsilon}_{2,2d} = \dot{\upsilon}_{2,2dm} + \dot{\upsilon}_{2,2du} + \frac{\partial\upsilon_{2,2d}}{\partial y}\tilde{x}_2 \tag{22}$$

In Eq. (22), $\dot{\upsilon}_{2,2dm}(t) \in \Re^1$ denotes the measurable components that are matched with the control input $\bar{\beta}(t)$ and can be done away with via direct cancellation, $\dot{\upsilon}_{2,2du}(t) \in \Re^1$ denotes immeasurable components that are linearly parameterizable and dealt with via the design of an adaptive update law, and the last term can be damped out because of the exponential stability of Eq. (16). (For explicit expressions for $\dot{\upsilon}_{2,2dm}(t)$ and $\dot{\upsilon}_{2,2du}(t)$, see Appendix A.) One can now write the open-loop dynamics for $e_2(t)$ in the following manner:

$$\dot{e}_2 = -k_2\upsilon_{2,1} + \upsilon_{2,3} + \bar{\beta} - \dot{\upsilon}_{2,2dm} - \frac{\partial\upsilon_{2,2d}}{\partial y}\tilde{x}_2 - \theta_2 e_1 + \boldsymbol{\omega}_2^T\boldsymbol{\sigma}_1 \tag{23}$$

where σ_1 and $\omega_2(t) \in \Re^{p2}$ denote, respectively, a vector of unknown constants and a measurable regression vector, and are explicitly defined in Appendix B. Motivated by the stability analysis and the structure of Eq. (23), the control input $\bar{\beta}(t)$ can be designed as follows:

$$\bar{\beta} = -c_{22}e_2 - d_{22}\left(\frac{\partial\upsilon_{2,2d}}{\partial y}\right)^2 e_2 - \upsilon_{2,3} + k_2\upsilon_{2,1} + \dot{\upsilon}_{2,2dm} - \boldsymbol{\omega}_2^T\hat{\boldsymbol{\sigma}}_1 \tag{24}$$

where c_{22} and d_{22} are positive gain constants. After this control input is substituted into Eq. (23), the closed-loop dynamics for $e_2(t)$ can be obtained in the following manner:

$$\dot{e}_2 = -c_{22}e_2 - d_{22}\left(\frac{\partial\upsilon_{2,2d}}{\partial y}\right)^2 e_2 - \frac{\partial\upsilon_{2,2d}}{\partial y}\tilde{x}_2 - \theta_2 e_1 + \boldsymbol{\omega}_2^T\tilde{\sigma}_1 \tag{25}$$

From the structure of Eq. (25), one can design a dynamic update law for $\hat{\sigma}_1(t)$ as $\dot{\hat{\sigma}}_1 = \omega_2 e_2$. For analyzing stability, a Lyapunov function

$$V = \frac{1}{2}\sum_{i=1}^{2} e_1^2 + \sum_{i=1}^{2} d_{ii}^{-1}\tilde{\boldsymbol{x}}^T P\tilde{\boldsymbol{x}} + \frac{|\theta_2|}{2}\tilde{\boldsymbol{\sigma}}_0^T\tilde{\boldsymbol{\sigma}}_0 + \tilde{\boldsymbol{\sigma}}_1^T\tilde{\boldsymbol{\sigma}}_1$$

is defined, the derivative of which along the closed-loop system dynamics yields the upper bound

$$\dot{V} \le -c_{11}e_1^2 - c_{22}e_2^2 - \tfrac{3}{4}\left(d_{11}^{-1} + d_{22}^{-1}\right)\tilde{\boldsymbol{x}}^T\tilde{\boldsymbol{x}} \tag{26}$$

through application of a nonlinear damping argument.[35] Following Ref. 34, signal chasing arguments can be used to state that $\lim_{t\to\infty} e_1(t)$ and $e_2(t) = 0$. From Eq. (16), the estimation error $\tilde{x}(t)$ is exponentially regulated to the origin.

V. Inclusion of Actuator Dynamics

To model the control surface dynamics along with the quasi-steady equations (1), the approach of Ref. 28 is followed, and a second-order system is assumed as follows:

$$\ddot{\beta} + p_1\dot{\beta} + p_2\beta = p_2 u, \qquad p_2 \neq 0 \tag{27}$$

where $\beta(t) \in \Re^1$ denotes the actual control surface deflection and $u(t)$ is the flap actuator output and the de facto control input signal. In this section, three different strategies are discussed to include the effect of the dynamics of the flap.

For the first strategy, let p_1 and p_2 be chosen such that the dynamics of Eq. (27) are faster than the dynamics of Eq. (1); then, similar to a cascaded control structure, the coupling of the plunge and pitch motion of the wing section can be neglected. The signal $\beta(t)$ introduced in Eq. (1) and designed subsequently in Eq. (24) can be treated as a desired flap deflection $\beta_d(t)$, and the control input $u(t)$ can be simply chosen to be

$$u(t) = \ddot{\beta}_d + p_1\dot{\beta}_d + p_2\beta_d \tag{28}$$

such that the closed-loop system for Eq. (27) becomes

$$\ddot{\varepsilon} + p_1\dot{\varepsilon} + p_2\varepsilon = 0 \tag{29}$$

which is an exponentially stable system, and where $\varepsilon \triangleq \beta - \beta_d$ denotes the error between the desired and actual flap deflection. Thus, $\beta(t)$ tracks $\beta_d(t)$ exponentially quickly.

However, if the actuator has slow dynamics, then one must consider the interconnection between the dynamics of Eqs. (1) and (27). One must then rewrite Eq. (23) as follows:

$$\dot{e}_2 = -k_2\upsilon_{2,1} + \upsilon_{2,3} + U^2\beta_d - \dot{\upsilon}_{2,2dm} - \frac{\partial\upsilon_{2,2d}}{\partial y}\tilde{x}_2 - \theta_2 e_1 + \boldsymbol{\omega}_2^T\boldsymbol{\sigma}_1 + U^2\varepsilon \tag{30}$$

Having designed $\beta_d(t)$ as done earlier in Eq. (24), it is easy to see that one is left with a $U^2\varepsilon$ mismatched indefinite term in the closed-loop dynamics for $\dot{e}_2(t)$. One can now represent the time derivative of $\varepsilon(t)$ as $\dot{\varepsilon} = \upsilon_\beta - \dot{\beta}_d$, where $\upsilon_\beta(t) \triangleq \dot{\beta}(t) \in \Re^1$. One can now define an auxiliary design variable $\eta_v(t) \in \Re^1$ as follows:

$$\eta_v = \upsilon_\beta - \upsilon_{\beta d}$$

where $\upsilon_{\beta d}(t)$ is a virtual control input that is chosen as follows:

$$\upsilon_{\beta d} = \dot{\beta}_d - U^2 e_2 + k_\varepsilon\varepsilon$$

such that the closed dynamics for $\dot{\varepsilon}(t)$ are obtained as follows:

$$\dot{\varepsilon} = -U^2 e_2 - k_\varepsilon\varepsilon + \eta_v$$

After time differentiating $\eta_v(t)$ and utilizing the actuator dynamics of Eq. (27), one can obtain

$$\dot{\eta}_v = -p_1\dot{\beta} - p_2\beta + p_2 u - \dot{\upsilon}_{\beta d}$$

Motivated by the structure of the foregoing open-loop dynamics, the control input signal can be designed as follows:

$$u(t) = p_2^{-1}[\dot{\upsilon}_{\beta d} + p_1\dot{\beta} + p_2\beta - \varepsilon - k_\eta\eta_v] \tag{31}$$

which yields a closed-loop form for the actuator dynamics as follows:

$$\dot{\eta}_v = -k_\eta\eta_v - \varepsilon$$

One can now augment the function V as $V_2 = V + \frac{1}{2}\varepsilon^2 + \frac{1}{2}\eta_v^2$, which yields, after differentiation along the system closed-loop trajectories, the following upper bound:

$$\dot{V}_2 \le -c_{11}e_1^2 - c_{22}e_2^2 - \tfrac{3}{4}\left(d_{11}^{-1} + d_{22}^{-1}\right)\tilde{\boldsymbol{x}}^T\tilde{\boldsymbol{x}} - k_\varepsilon\varepsilon^2 - k_\eta\eta_v^2$$

Again, a signal chasing argument would show that $\lim_{t\to\infty} e_1(t), e_2(t), \tilde{\boldsymbol{x}}(t)$, and $r(t) = 0$. Note that the augmentation strategy involves two derivatives of $\beta_d(t)$, which certainly leads to measurements of more variables than was stated earlier. With a great deal of extra work, one could work around making the extra measurements; however, that will not be pursued here in the interest of brevity. Also note that there was a need to utilize measurements of the state variables $\beta(t)$ and $\dot{\beta}(t)$, as well as the model parameters p_1 and p_2. To mitigate this dependence and design a true output feedback control strategy with measurements of only the pitch displacement, as well as to compensate adaptively for uncertainty in p_1 and p_2, one would need to redesign comprehensively the estimation, adaptation, and control strategies. The methodology followed in this paper would still be valid, but the estimation strategy would have to include observers for the new states, that is, $\beta_1(t)$ and its time derivative. Additionally, the parameter update laws would need to be augmented to compensate for the effects of the actuator model in terms of p_1 and p_2.

VI. Results and Discussion

The model described in Eq. (3) was simulated using the observation and control algorithm of Eqs. (12–14) and (24). The values for the model parameters were taken from Ref. 19 and are listed hereafter,

$$b = 0.135\ \text{m}, \qquad k_h = 2844.4\ \text{N}\cdot\text{m}^{-1}, \qquad c_h = 27.43\ \text{N}\cdot\text{m}^{-1}\cdot\text{s}^{-1}$$

$$c_\alpha = 0.036\ \text{N}\cdot\text{s}, \qquad \rho = 1.225\ \text{kg}\cdot\text{m}^3, \qquad c_{l\alpha} = 6.28$$

$$c_{l\beta} = 3.358, \qquad c_{m\alpha} = (0.5 + a)c_{l\alpha}, \qquad c_{m\beta} = -0.635$$

$$m = 12.387\ \text{kg}, \qquad I_\alpha = 0.065\ \text{kg}\cdot\text{m}^2$$

$$x_\alpha = [0.0873 - (b + ab)]/b, \qquad a = -0.4 \tag{32}$$

The nonlinear pitch spring stiffness was represented by a quintic polynomial as follows:

$$k_y(y) = \sum_{i=1}^{5} \tau_i y^{i-1} \tag{33}$$

where the unknown τ_i extracted from experimental data[20] are given as

$$\{\tau_i\} = [2.8 \quad -62.3 \quad 3709.7 \quad -24{,}195.6 \quad 48{,}756.9]^T$$

The first simulation was run with freestream velocity $U = 20\ \text{m}\cdot\text{s}^{-1}$, whereas the initial conditions for the system states, observed variables, and estimates were chosen as follows:

$$\alpha(0) = 0.1\ \text{rad}, \qquad \dot{\alpha}(0) = 0\ \text{rad}\cdot\text{s}^{-1}, \qquad h(0) = 0\ \text{m}$$

$$\dot{h}(0) = 0\ \text{m}\cdot\text{s}^{-1}, \qquad \hat{\sigma}_0(0) = 0, \qquad \hat{\sigma}_1(0) = 0$$

$$\zeta_0(0) = 0, \qquad \zeta_j(0) = 0, \qquad \upsilon_j(0) = 0 \tag{34}$$

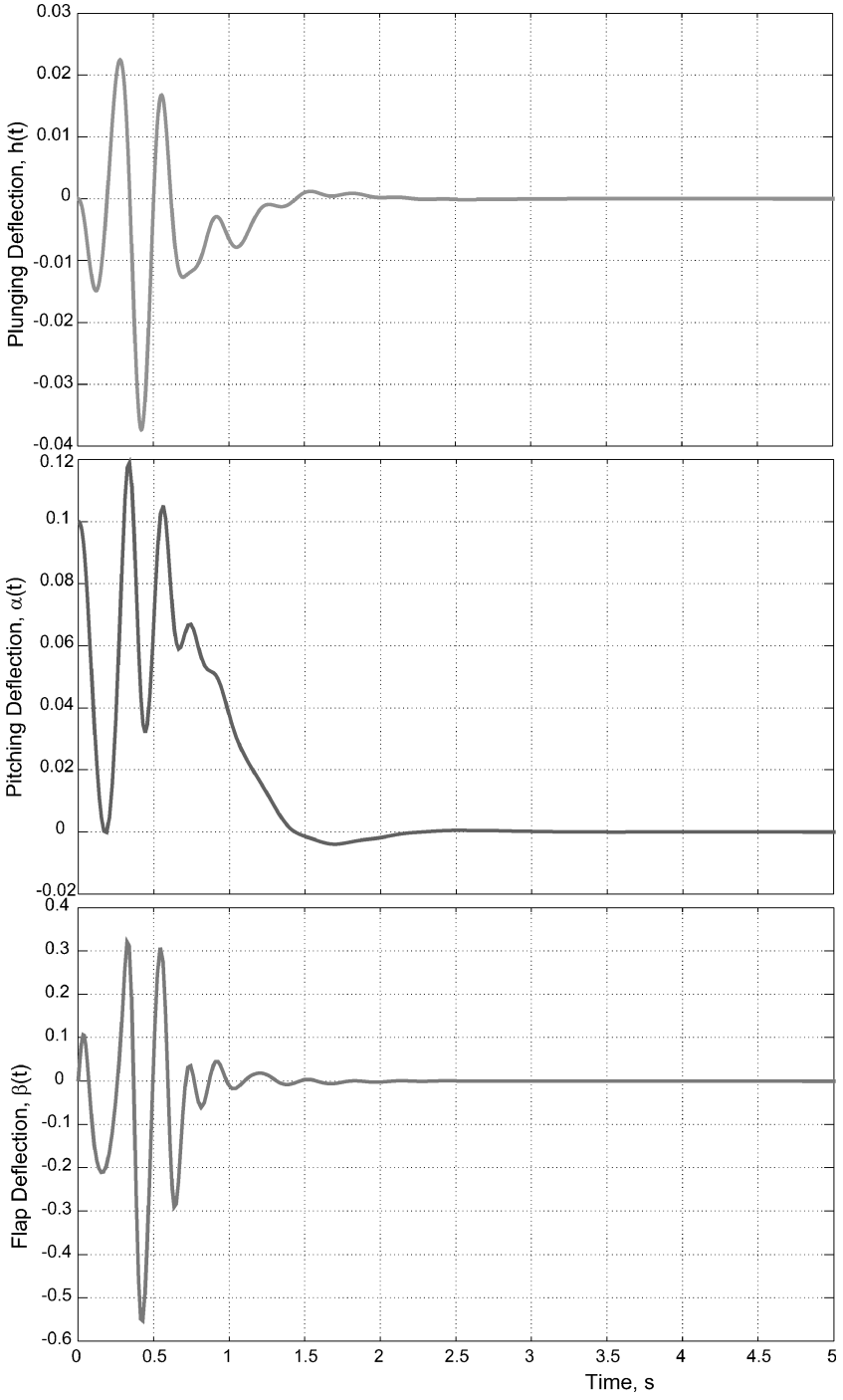

Fig. 2 Time evolution of closed-loop plunging and pitching deflections and flap deflection for $U = 20$ [m · s^{-1}]; $U = 1.6U_{\text{flutter}}$.

Figure 2 shows the closed-loop plunging, pitching, and control surface deflection time histories for the case when the actuation is on at time zero. In the presence of active control, the system states are regulated to the origin fairly rapidly. Note that the adaptive control strategy is able to regulate quickly the plunging and pitching response in the presence of large uncertainty in the parameters. The second simulation was run with freestream velocity $U = 15$ m · s^{-1} with the same initial conditions as Eq. (34). However, in this case, the system is allowed to evolve as open loop, that is, $\beta(t) \equiv 0$, for 15 s, to observe the development of an LCO. During the first 15 s, the estimation strategy is allowed to evolve according to the dynamics of Eqs. (12–14). Because the observation strategy is independent of control design, it can be allowed to evolve even when the system is working in an open-loop fashion. This is because the observation error is exponentially stable independent of what control is chosen. However, the parameter estimation strategy is turned off because of its dependence on the control strategy of Eq. (24). This is because parameter estimators are designed in conjunction with the closed-loop controller, and so the stability of these estimators is dependent on the particular choice of control strategy. When the system is working in open-loop fashion, that is, the controller is off, then these estimators also need to be turned off, otherwise they would turn unstable, and the simulation would not complete. At $t = 15$ s, the control is turned on, and the immediate attenuation of oscillations can be seen in Figs. 3 and 4. Again, the response is seen to be quick in the presence of large model uncertainty. Figure 5 shows a comparison with the results of Ref. 28 for controlled pitch response of LCO behavior for the nonlinear aeroelastic system with $\alpha(0) = 0.087$ rad, $h(0) = 0$ rad, and $U = 16$ m · s^{-1}. The LCOs occur at approximately 50.83 ft · s^{-1} (15.25 m · s^{-1}) and at a frequency of 2.87 Hz, which is

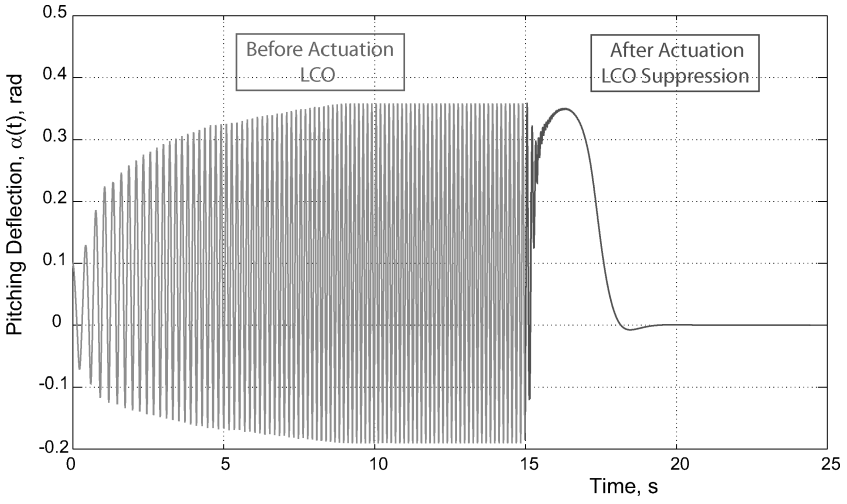

Fig. 3 Time history of pitching deflection for $U = 15\ \mathrm{m \cdot s^{-1}}$, $U = 1.25U_{\mathrm{flutter}}$.

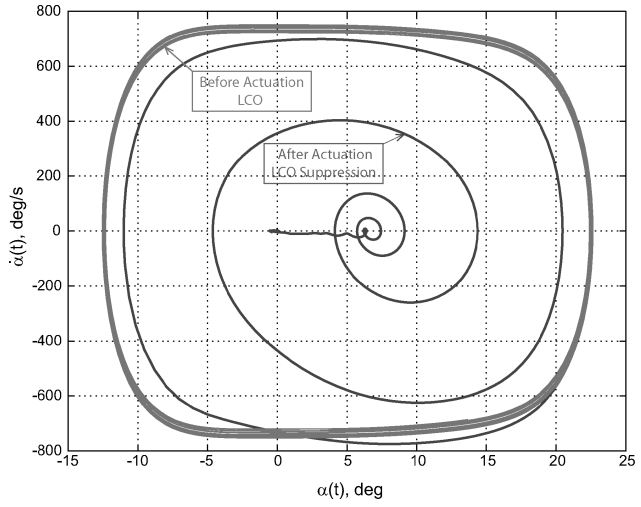

Fig. 4 Phase space of pitching deflection for $U = 15\ \mathrm{m \cdot s^{-1}}$, $U = 1.25U_{\mathrm{flutter}}$.

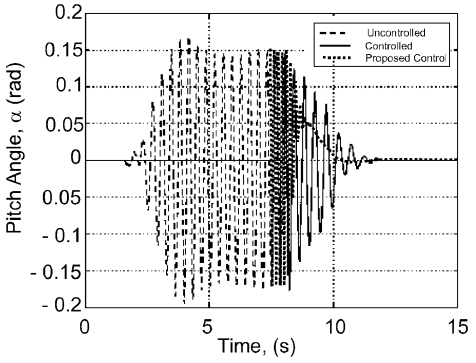

Fig. 5 Comparison of pitching time history vs optimal observer with full-state feedback.[28]

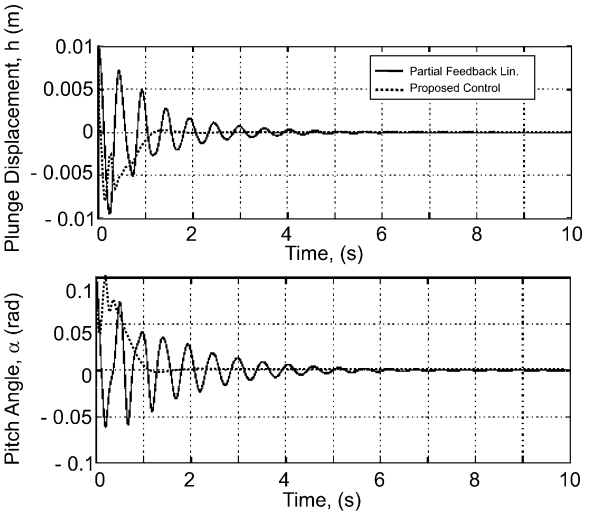

Fig. 6 Comparison of plunging and pitching time history vs nonlinear partial feedback linearization technique.[19]

in agreement with the results of Ref. 28. The comparison of predictions for the closed-loop response shows that the control technique presented in this paper very effectively suppresses the LCO. The optimal observer and full-state feedback implemented in Ref. 28 is effective only near the flutter velocity, but it seems that the control law will not suppress the instability at higher speed. From results not displayed here, it appears that the present control is also very effective at higher speeds. A comparison with the results obtained via a nonlinear partial feedback linearization technique by Ko et al.[19] is also presented in Fig. 6. Again, the vibrations are effectively suppressed, and the closed-loop response has a fast settling time. The initial conditions are chosen as in Ref. 19, as follows: $\alpha(0) = 0.1$ rad, and $h(0) = 0.01$ m. The performance of the model free adaptive control is also compared with the result by Kim and Crassidis[36] in Fig. 7. The nominal controller in Ref. 36 fails to stabilize the response without model-error control synthesis (MECS); with MECS, the LCO is stabilized, and the vibrations are reduced to 5% of the maximum amplitude within 6–8 s. The initial conditions are chosen as in Ref. 36, as follows: $\alpha(0) = 0$ rad, and $h(0) = -0.02$ m. The comparison shows that our proposed control is very effective in that the vibrations are suppressed to within 1% of the maximum vibration amplitude in less than 2 s. Note that the model used to generate data for Figs. 2–7 does not contain actuator dynamics so that comparisons can be made with data existing in the literature.

In Fig. 8 comparison is made for the pitch, plunging, and actuation response between the control strategy of Eq. (24) with no actuator dynamics and the strategy of Eq. (28), where fast actuator dynamics are assumed to exist. From Fig. 8, note that when the actuation is introduced with fast actuator dynamics, the difference in pitching time history is imperceptible from when there are no dynamics. This is to be expected, because the poles of the actuation dynamics do not interact with the closed-loop poles of the pitching and plunging dynamics. However, the inclusion of slow actuator dynamics was seen to degrade transient performance when these dynamics were added

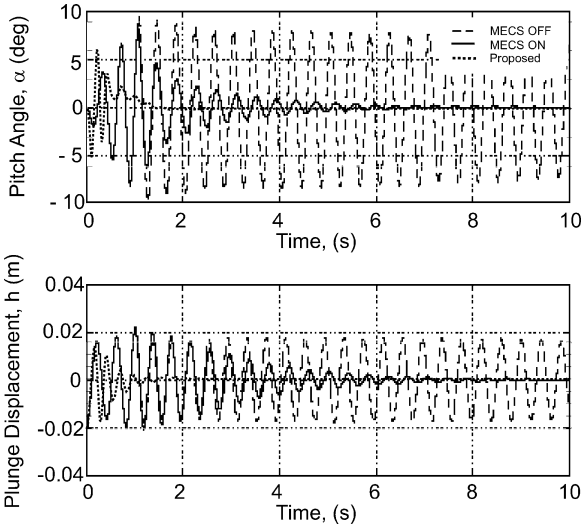

Fig. 7 Comparison of plunging and pitching time history vs MECS.[36]

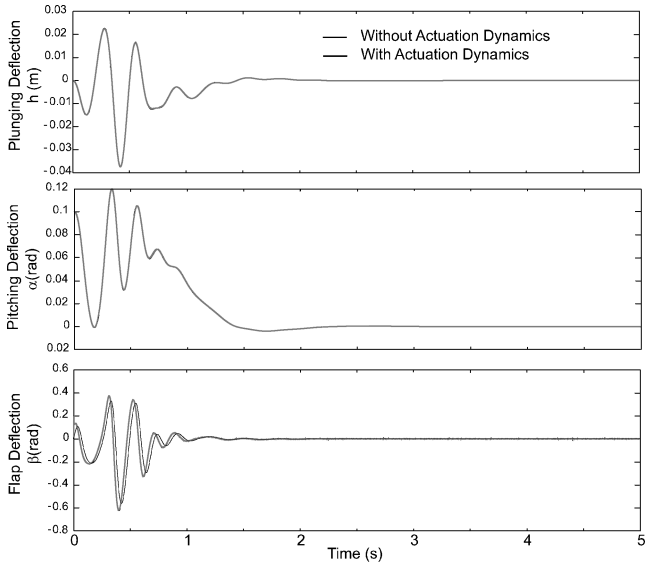

Fig. 8 Closed-loop aeroelastic responses with and without actuation dynamics.

to the model without actuation dynamics. The authors believe that this interaction between the poles of the two systems calls for a retuning of the controller parameters to recover the dynamic performance.

Note that the methodology presented here can be extended to the compressible flight speed regimes. In this sense, pertinent aerodynamics for the compressible subsonic, supersonic, and hypersonic flight speed regimes have to be applied.[37] However, the goal of this paper was restricted to the issue of the illustration of the methodology and to that of highlighting the importance of the implementation of the nonlinear adaptive control on the lifting surfaces equipped with a flap.

VII. Conclusions

In this paper, a true output feedback strategy (that utilizes only measurements of the pitching variable α) has been obtained for the adaptive control of a nonlinear plunging–pitching wing section operating in an incompressible flight speed. A quasi-steady aerodynamic model is used, and an unsteady one is contemplated for future work. The performance of the adaptive controller is analyzed with and without actuation dynamics. It clearly appears that the controller is able to control the LCO efficiently.

Although the formulation of the state estimation strategy, as well as the adaptive control design, seems at first to be complicated, this formulation is very systematic and can be extended to complex aeroelastic problems in a systematic fashion. The relevance of this paper is not in designing a complicated controller for a very simple system, but the way that this methodology can be extended in an algorithmic fashion for all aeroelastic systems that can be obtained in the output feedback form with nonlinearity only in the output variable.

Most controllers are designed by linearizing a system about a set of operating conditions. The separation principle is then used to design a state estimator. However, the aeroelastic system loses the LCO beyond flutter speed when system is linearized. Therefore, one must preserve the nonlinearity. Doing so, one is unable to use the separation principle from linear systems theory. Thus, the choice is to go with state feedback design, but that is impractical with the limited amount of sensing that is available. Therefore, one must design an output feedback strategy that is comprehensive and guarantees stability. Additionally, one cannot be expected to know all parameters of the model; this controller compensates for uncertainty in those parameters. Although we do not guarantee estimation of all parameters, we can guarantee stability even when the parameters are off from their nominal values.

Because the controller is nonlinear and adaptive, a potential weakness of this paper is the large space of controller and estimator parameters that needs to be explored by the design engineer to map the parameters to transient and steady-state design specifications.

Appendix A: Aeroelastic Model Constants and State Feedback Coefficients

The auxiliary constants k_i and $c_i \forall i = 1, \ldots, 4$, as well as g_3 and g_4 that were introduced in the model description (4), are explicitly defined as follows:

$$k_1 = I_\alpha k_h d^{-1}, \qquad k_2 = d^{-1}\left[I_\alpha \rho b c_{l\alpha} + m x_\alpha b^3 \rho c_{m\alpha}\right]$$

$$k_3 = -m x_\alpha b k_h d^{-1}, \qquad k_4 = d^{-1}\left[-m x_\alpha b^2 \rho c_{l\alpha} - m\rho b^2 c_{m\alpha}\right]$$

$$c_1 = d^{-1}\left[I_\alpha\left(c_h + \rho U b c_{l\alpha}\right) + m x_\alpha \rho U b^3 c_{m\alpha}\right]$$

$$c_2 = d^{-1}\left[I_\alpha \rho U b^2 c_{l\alpha}\bar{a} - m x_\alpha b c_\alpha + m x_\alpha \rho U b^4 c_{m\alpha}\bar{a}\right]$$

$$c_3 = d^{-1}\left[-m x_\alpha b c_h - m x_\alpha \rho U b^2 c_{l\alpha} - m\rho U b^2 c_{m\alpha}\right]$$

$$c_4 = d^{-1}\left[m c_\alpha - m x_\alpha \rho U b^3 c_{l\alpha}\bar{a} - m\rho U b^3 c_{m\alpha}\bar{a}\right]$$

$$g_3 = d^{-1}\left[-I_\alpha \rho b c_{l\beta} - m x_\alpha b^3 \rho c_{m\beta}\right]$$

$$g_4 = d^{-1}\left[m x_\alpha b^2 \rho c_{l\beta} + m\rho b^2 c_{m\beta}\right]$$

$$d = m\left(I_\alpha - m x_\alpha^2 b^2\right), \qquad \bar{a} = (0.5 - a)$$

The elements $\theta_i \forall i = 2, 3, 4$ introduced in Eq. (17) are explicitly defined as follows:

$$\theta_2 = g_4, \qquad \theta_3 = -g_3 c_3 + c_1 g_4$$

$$\theta_4 = k_1 g_4 + k_1 c_3^2 g_3 k_3^{-1} - c_1 g_3 c_3 - d_{obs} g_3 k_3^{-1} \tag{A1}$$

Given the pitch spring constant of Eq. (33), explicit expression for $\boldsymbol{W}(y)$ and $\boldsymbol{\gamma}$ introduced in Eq. (8) are

$$\boldsymbol{W}(y) = \begin{bmatrix} y & 0 & 0 & 0 & 0 & 0 & 0 & 0 & 0 & 0 & 0 & 0 & 0 & 0 & 0 & 0 \\ 0 & y & 0 & 0 & y^2 & 0 & 0 & y^3 & 0 & 0 & y^4 & 0 & 0 & y^5 & 0 & 0 \\ 0 & 0 & y & 0 & 0 & y^2 & 0 & 0 & y^3 & 0 & 0 & y^4 & 0 & 0 & y^5 & 0 \\ 0 & 0 & 0 & y & 0 & 0 & y^2 & 0 & 0 & y^3 & 0 & 0 & y^4 & 0 & 0 & y^5 \end{bmatrix} \tag{A2}$$

$$\gamma_1 = \delta_1, \qquad \gamma_2 = \delta_2 + \left(-k_4 U^2 - m d^{-1}\tau_1\right)$$

$$\gamma_3 = \delta_3 + c_3 k_2 U^2 - c_1 k_4 U^2 - m x_\alpha b \tau_1 c_3 d^{-1} - c_1 m \tau_1 d^{-1}$$

$$\gamma_4 = -k_1k_4U^2 - k_1md^{-1}\tau_1 + k'k_2U^2 - k'mx_\alpha bd^{-1}\tau_1$$
$$\gamma_5 = -\tau_2md^{-1}, \qquad \gamma_6 = -\tau_2\left(c_3mx_\alpha bd^{-1} + c_1md^{-1}\right)$$
$$\gamma_7 = -\tau_2\left(k_1md^{-1} + k'mx_\alpha bd^{-1}\right), \qquad \gamma_8 = -\tau_3md^{-1}$$
$$\gamma_9 = -\tau_3\left(k_1md^{-1} + k'mx_\alpha bd^{-1}\right)$$
$$\gamma_{10} = -\tau_3\left(k_1md^{-1} + k'mx_\alpha bd^{-1}\right)$$
$$\gamma_{11} = -\tau_4md^{-1}, \qquad \gamma_{12} = -\tau_4\left(k_1md^{-1} + k'mx_\alpha bd^{-1}\right)$$
$$\gamma_{13} = -\tau_4\left(k_1md^{-1} + k'mx_\alpha bd^{-1}\right), \qquad \gamma_{14} = -\tau_5md^{-1}$$
$$\gamma_{15} = -\tau_5\left(k_1md^{-1} + k'mx_\alpha bd^{-1}\right)$$
$$\gamma_{16} = -\tau_5\left(k_1md^{-1} + k'mx_\alpha bd^{-1}\right) \tag{A3}$$

where k' and $\delta_i \in \Re$ are defined as follows:

$$\delta_1 = -c_1 - c_4, \qquad \delta_2 = c_2c_3 - k_1 - c_1c_4$$
$$\delta_3 = k_3^{-1}\left[-k_1c_4c_5 - k_1c_2c_3^2 - c_1c_3c_4k_1 + c_1c_2c_3k_3 + d_{obs}c_2\right]$$
$$k' = k_3^{-1}\left[c_1c_3k_3 - k_1c_3^2 + d_{obs}\right] \tag{A4}$$

Noted here that it is simple to alter the size and definition of γ if it is desired that the freestream velocity U be a part of the measurable regression vector $W(\,)$ of Eq. (8).

The vector of unknown constants $\boldsymbol{\sigma}_0 \in \Re^{p1}$ and the measurable regression vector $\boldsymbol{\omega}_1(t) \in \Re^{p1}$ utilized in Eq. (18) are explicitly defined as follows:

$$\boldsymbol{\sigma}_0^T = \left[\theta_2^{-1} \quad \theta_2^{-1}\gamma_1 \quad \theta_2^{-1}\gamma_2 \quad \cdots \quad \theta_2^{-1}\gamma_p \quad \theta_2^{-1}\theta_3 \quad \theta_2^{-1}\theta_4\right]$$
$$\boldsymbol{\omega}_1^T = [c_{11}e_1 + d_{11}e_1 + \zeta_{0,2} \quad \zeta_{1,2} + W_{1,1}(y) \quad \zeta_{2,2} + W_{2,1}(y) \quad \cdots \quad \zeta_{p,2} + W_{p,1}(y) \quad \upsilon_{3,2} \quad \upsilon_{4,2}]$$

The vector of unknown constants $\boldsymbol{\sigma}_1 \in \Re^{p2}$ and the measurable regression vector $\boldsymbol{\omega}_2(t) \in \Re^{p2}$ utilized in Eq. (23) are explicitly defined as follows:

$$\boldsymbol{\sigma}_1^T = [\gamma_1 \quad \gamma_2 \quad \cdots \quad \gamma_p \quad \theta_2 \quad \theta_3 \quad \theta_4]$$
$$\boldsymbol{\omega}_2^T = \left\{-\frac{\partial \upsilon_{2,2d}}{\partial y}[\zeta_{1,2} + W_{1,1}(y)] \quad \cdots \quad -\frac{\partial \upsilon_{2,2d}}{\partial y}[\zeta_{p,2} + W_{p,1}(y)] \quad -\frac{\partial \upsilon_{2,2d}}{\partial y}\upsilon_{2,2} + e_1 \quad \upsilon_{3,2} \quad \upsilon_{4,2}\right\}$$

The explicit expressions for $\dot{\upsilon}_{2,2dm}(t)$ and $\dot{\upsilon}_{2,2du}(t)$ are obtained as follows:

$$\dot{\upsilon}_{2,2dm} = \frac{\partial \upsilon_{2,2d}}{\partial y}\zeta_{02} + \frac{\partial \upsilon_{2,2d}}{\partial \zeta_0}[\boldsymbol{A}_0\boldsymbol{\zeta}_0 + ky]$$
$$+ \sum_{j=1}^{p}\frac{\partial \upsilon_{2,2d}}{\partial \zeta_j}[\boldsymbol{A}_0\boldsymbol{\zeta}_j + \boldsymbol{W}_j(y)]$$
$$+ \sum_{j=3}^{4}\frac{\partial \upsilon_{2,2d}}{\partial \upsilon_j}\boldsymbol{A}_0\boldsymbol{\upsilon}_j + \frac{\partial \upsilon_{2,2d}}{\partial \hat{\sigma}_0}[\text{sign}(\theta_2)\omega_1e_1]$$
$$\dot{\upsilon}_{2,2du} = \frac{\partial \upsilon_{2,2d}}{\partial y}\left(\sum_{j=1}^{p}\gamma_j[\zeta_{j,2} + W_{j,1}(y)] + \sum_{j=2}^{4}\theta_j\upsilon_{j,2}\right)$$

Appendix B: Stability of the Zero Dynamics

The state-space system (6) can be expanded into the following form:

$$y = x_1 = \alpha, \qquad \dot{x}_1 = x_2 + \Phi_1(y), \qquad \dot{x}_2 = x_3 + \Phi_2(y) + \theta_2\bar{\beta}$$
$$\dot{x}_3 = x_4 + \Phi_3(y) + \theta_3\bar{\beta}, \qquad \dot{x}_4 = \Phi_4(y) + \theta_4\bar{\beta} \tag{B1}$$

Here, the stability of the zero dynamics is studied for the case when the pitch displacement is regulated to the origin. Mathematically, this implies that

$$y \equiv 0 \Rightarrow \dot{y} = x_2 \equiv 0 \Rightarrow \dot{x}_2 \equiv 0$$

which implies from the second equation (B1) that

$$u^* = (1/\theta_2)[-x_3 + \Phi_2(0)] \tag{B2}$$

From Eq. (A2), it is plain to see that $W(0) = 0$, which implies that $\Phi_i(0) = 0\,\forall\, i = 1, \ldots, 4$. The zero dynamics of the system then reduce to the second-order system given by

$$\dot{x}_3 = x_4 + \theta_3u^*, \qquad \dot{x}_4 = \theta_4u^*$$

When Eq. (B2) is substituted into the preceding set of equations for u^*, the linear system of equations $\dot{\boldsymbol{x}} = \boldsymbol{A}^*\boldsymbol{x}$ can be obtained, where $\boldsymbol{x} = [x_3 \;\; x_4]^T$ and A^* is given by

$$A^* = \begin{bmatrix} -\dfrac{\theta_3}{\theta_2} & 1 \\ -\dfrac{\theta_4}{\theta_2} & 0 \end{bmatrix}$$

The eigenvalues of which are given by

$$\lambda_{A^*} = (1/2\theta_2)\left(-\theta_3 \pm \sqrt{\left(\theta_3^2 - 4\theta_2\theta_4\right)}\right)$$

From the nominal system (32) and the expressions (A1), one can compute $\theta_2 = -0.1655$, $\theta_3 = -0.6275$, and $\theta_4 = -50.4645$, from which $\text{Re}(\lambda_A) = -1.8958$, which gives asymptotically stable zero dynamics. For the sake of completeness, we mention that the eigenvalues for the zero dynamics turn out to be $\lambda_A = -1.8958 \pm j5.7458$.

Acknowledgments

The authors thank Anup Lonkar for developing the initial simulation framework. The authors also acknowledge the critiques of the reviewers and the editor that served to shape the content and flow of the manuscript.

References

[1]Dowell, E. H., *A Modern Course in Aeroelasticity*, Sijthoff and Noordhoff, 1978.

[2]Marzocca, P., Librescu, L., and Chiocchia, G., "Aeroelastic Response of a 2-D Lifting Surfaces to Gust and Arbitrary Explosive Loading Signatures," *International Journal of Impact Engineering*, Vol. 25, No. 1, 2001, pp. 41–65.

[3]Marzocca, P., Librescu, L., and Chiocchia, G., "Aeroelasticity of Two-Dimensional Lifting Surfaces via Indicial Function Approach," *Aeronautical Journal*, Vol. 106, No. 1056, 2002, pp. 147–153.

[4]Marzocca, P., Librescu, L., and Silva, W. A., "Nonlinear Open-/Closed-Loop Aeroelastic Analysis of Airfoils via Volterra Series," *AIAA Journal*, Vol. 42, No. 4, 2004, pp. 673–686.

[5]Vipperman, J. S., Clark, R. L., Conner, M. D., and Dowell, E. H., "Investigation of the Experimental Active Control of a Typical Section Airfoil Using a Trailing-Edge Flap," *Journal of Aircraft*, Vol. 35, No. 2, 1998, pp. 224–229.

[6]Lazaraus, K., Crawley, E., and Lin, C., "Fundamental Mechanisms of Aeroelastic Control with Control Surface and Strain Actuation," *Journal of Guidance, Control, and Dynamics*, Vol. 18, No. 1, 1995, pp. 10–17.

[7]Mukhopadhyay, V. (ed.), "Benchmark Active Control Technology," Pt. 1, *Journal of Guidance, Control, and Dynamics*, Vol. 23, No. 5, 2000, pp. 913–960.

[8]Mukhopadhyay, V. (ed.), "Benchmark Active Control Technology," Pt. 2, *Journal of Guidance, Control, and Dynamics*, Vol. 23, No. 6, 2000, pp. 1093–1139.

[9]Mukhopadhyay, V. (ed.), "Benchmark Active Control Technology," Pt. 3, *Journal of Guidance, Control, and Dynamics*, Vol. 24, No. 1, 2001, pp. 146–192.

[10]Mukhopadhyay, V., "Historical Perspective on Analysis and Control of Aeroelastic Responses," *Journal of Guidance, Control, and Dynamics,* Vol. 26, No. 5, 2003, pp. 673–684.

[11]Yuan, Y., Yu, P., Librescu, L., and Marzocca, P., "Aeroelasticity of Time-Delayed Feedback Control of Two-Dimensional Supersonic Lifting Surfaces," *Journal of Guidance, Control, and Dynamics*, Vol. 27, No. 5, 2004, pp. 795–803.

[12]Dowell, E. H., Edwards, J., and Strganac, T., "Nonlinear Aeroelasticity," *Journal of Aircraft*, Vol. 40, No. 5, 2003, pp. 857–874.

[13]Jones, D. J., and Lee, B. H. K., "Time Marching Numerical Solution of the Dynamic Response of Nonlinear Systems," National Aeronautical Establishment, Aeronautical Note–25, National Research Council, Ottawa, 1985.

[14]Friedmann, P., Guillot, D., and Presente, E., "Adaptive Control of Aeroelastic Instabilities in Transonic Flow and Its Scaling," *Journal of Guidance, Control, and Dynamics*, Vol. 20, No. 6, 1997, pp. 1190–1199.

[15]Lind, R., and Brenner, M., *Robust Aeroservoelastic Stability Analysis*, Springer-Verlag, London, 1999.

[16]Barker, J. M., and Balas, G. J., "Comparing Linear Parameter-Varying Gain-Scheduled Control Techniques for Active Flutter Suppression," *Journal of Guidance, Control, and Dynamics*, Vol. 23, No. 5, 2000, pp. 948–955.

[17]Scott, R. C., and Pado, L. E., "Active Control of Wind-Tunnel Model Aeroelastic Response Using Neural Networks," *Journal of Guidance, Control, and Dynamics*, Vol. 23, No. 6, 2000, pp. 1100–1108.

[18]Guillot, D. M., and Friedmann, P. P., "Fundamental Aeroservoelastic Study Combining Unsteady Computational Fluid Mechanics with Adaptive Control," *Journal of Guidance, Control, and Dynamics*, Vol. 23, No. 6, 2000, pp. 1117–1126.

[19]Ko, J., Kurdila, A. J., and Strganac, T. W., "Nonlinear Control of a Prototypical Wing Section with Torsional Nonlinearity," *Journal of Guidance, Control, and Dynamics*, Vol. 20, No. 6, 1997, pp. 1181–1189.

[20]Ko, J., and Strganac, T. W., "Stability and Control of a Structurally Nonlinear Aeroelastic System," *Journal of Guidance, Control, and Dynamics*, Vol. 21, No. 5, 1998, pp. 718–725.

[21]Ko, J., Strganac, T. W., and Kurdila, A. J., "Adaptive Feedback Linearization for the Control of a Typical Wing Section with Structural Nonlinearity," *Nonlinear Dynamics*, Vol. 18, No. 3, 1999, pp. 289–301.

[22]Zeng, Y., and Singh, S. N., "Output Feedback Variable Structure Adaptive Control of an Aeroelastic Systems," *Journal of Guidance, Control, and Dynamics*, Vol. 21, No. 6, 1998, pp. 830–837.

[23]Singh, S. N., and Wang, L., "Output Feedback Form and Adaptive Stabilization of a Nonlinear Aeroelastic System," *Journal of Guidance, Control, and Dynamics*, Vol. 25, No. 4, 2002, pp. 725–732.

[24]Xing, W., and Singh, S. N., "Adaptive Output Feedback Control of a Nonlinear Aeroelastic Structure," *Journal of Guidance, Control, and Dynamics*, Vol. 23, No. 6, 2000, pp. 1109–1116.

[25]Zhang, R., and Singh, S. N., "Adaptive Output Feedback Control of an Aeroelastic System with Unstructured Uncertainties," *Journal of Guidance, Control, and Dynamics*, Vol. 24, No. 3, 2001, pp. 502–509.

[26]Scanlan, R. H., and Rosenbaum, R., *Introduction to the Study of Aircraft Vibration and Flutter*, Macmillan, New York, 1951.

[27]Edwards, J. W., "Unsteady Aerodynamic Modeling and Active Aeroelastic Control," Guidance and Control Lab., Dept. of Aeronautics and Astronautics, SUDARR 504, Stanford Univ., Stanford, CA, Feb. 1977; also NASA CR-148019, 1977.

[28]Block, J. J., and Strganac, T. W., "Applied Active Control for a Nonlinear Aeroelastic Structure," *Journal of Guidance, Control, and Dynamics*, Vol. 21, No. 6, 1998, pp. 838–845.

[29]Fung, Y. C., *An Introduction to the Theory of Aeroelasticity*, Dover, New York, 1955.

[30]Leishman, J. G., "Unsteady Lift of an Airfoil with a Trailing-Edge Flap Based on Indicial Concepts," *Journal of Aircraft*, Vol. 31, No. 2, 1994, pp. 288–297.

[31]Leishman, J. G., "Validation of Approximate Indicial Aerodynamic Functions for Two-Dimensional Subsonic Flow," *Journal of Aircraft*, Vol. 25, No. 2, 1988, pp. 914–922.

[32]Marzocca, P., Librescu, L., and Chiocchia, G., "Aeroelastic Response of a 2-D Airfoil in Compressible Flight Speed Regimes Exposed to Blast Loadings," *Aerospace Science and Technology*, Vol. 6, No. 3, 2002, pp. 259–272.

[33]Qin, Z., Marzocca, P., and Librescu, L., "Aeroelastic Instability and Response of Advanced Aircraft Wings at Subsonic Flight Speeds," *Aerospace Science and Technology*, Vol. 6, No. 5, 2002, pp. 195–208.

[34]Krstić, M., Kanellakopoulos, I., and Kokotović, P., *Nonlinear and Adaptive Control Design*, Wiley, New York, 1995.

[35]Kokotovic, P., "The Joy of Feedback: Nonlinear and Adaptive," *Institute of Electrical and Electronic Engineers Control Systems Magazine*, Vol. 12, June 1992, pp. 7–17.

[36]Kim, J., and Crassidis, J. L., "Limit Cycle Oscillation Control of Aeroelastic Systems Using Model-Error Control Synthesis," AIAA Paper 2003-5506, Aug. 2003.

[37]Bisplinghoff, R. L., Ashley, H., and Halfman, R. L., *Aeroelasticity*, Dover, New York, 1996, Chap. 6.